Buenos Aires – 5 to 9 September, 2016
Acoustics for the 21st Century…

PROCEEDINGS of the 22nd International Congress on Acoustics

Hearing Protectors: Paper ICA2016-98

Using finite–element modeling to predict the effect of sound incidence on the Noise Reduction based attenuation of earmuffs

Sgard Franck[(a)], Gaudreau Marc-André[(b)], Nélisse Hugues[(c)]

[(a)] Institut de recherche Robert-Sauvé en santé et en sécurité du travail (IRSST), Canada, frasga@irsst.qc.ca
[(b)] École de Technologie Supérieure, Canada, mgaudreau@etsmtl.ca
[(c)] IRSST, Canada, hugnel@irsst.qc.ca

Abstract

The sound attenuation of Hearing Protector Devices (HPD) can be measured objectively using the “Microphone In the Real Ear” (MIRE) method or with its field counterpart, the F-MIRE method. This two microphone method, with one microphone outside and the other inside the HPD, can be used to evaluate the attenuation in the form of a noise reduction (NR) obtained from the difference between the sound pressure levels at the two microphones. Correction factors, based usually on diffuse field or frontal incidence, can be applied on NR values to obtain an estimate of the insertion loss (IL) of the HPD, a more common measure of the sound attenuation. The F-MIRE method has been used for continuous measurements on earmuffs in real field environments where the sound field can depart significantly from a diffuse field and may show strong directionalities. These field attenuation measurements have been shown to depend on the direction of the incoming sound, therefore, asking for a revision of the correction factors. Obtaining experimentally these factors that depend on both the external and internal microphone positions together with the incidence angle is cumbersome. This paper uses a 3D finite element model of an Acoustic Test Fixture (ATF) with and without earmuff, excited acoustically at various angles of incidence to calculate the correction factors. To assess the validity of the model, the simulated attenuation results are compared with experimental measurements on an ATF equipped with an earmuff placed in an anechoic room for various incidence angles. The effect on the correction factors of the angle of incidence together with the positions of the external and internal microphones is then simulated and discussed.

Keywords: hearing protection

Using finite–element modeling to predict the effect of sound incidence on the Noise Reduction based attenuation of earmuffs

1 Introduction

The sound attenuation of hearing protectors devices (HPD) can be measured subjectively using the "gold standard" attenuation measurement method called the real-ear attenuation at threshold (REAT)[1]. This method is based on the assessment of the differences between the open and occluded ear auditory thresholds measured in a very quiet standardized acoustic environment. Alternatively, the sound attenuation of HPDs can be assessed objectively in laboratory using "Microphone In the Real Ear" (MIRE) [2] method or in the field using "Field-MIRE" method. In the MIRE technique, the sound attenuation of HPDs is quantified using the insertion loss (IL) defined as the difference of sound pressure levels (SPL) measured at the eardrum with and without the HPD. This requires two separate measurements. The Field-MIRE method utilizes two microphones (one on each side of the HPD) and provides an indicator called the measured noise reduction (NR^*) defined as the difference between the SPL outside and underneath the HPD and which is obtained in a single measurement. In practice the inner microphone is often placed inside the earcup volume close to the ear canal entrance. All these methods have pros and cons and lead to different attenuation results. However, these attenuation data can be compared by introducing correction factors derived from ensemble averages which relate the REAT, IL and NR^* attenuation values [3]. The relations linking these psychoacoustical and physical attenuation values are given by:

$$REAT = IL + PN \tag{1}$$

$$IL = NR^* + TF'_{canal} - TF'_{ext} + TFOE \tag{2}$$

where IL is the insertion loss measured with an inner microphone positioned at eardrum, PN denotes the physiological noise, NR^* is the noise reduction measured between an external microphone and the inner microphone positioned underneath the protector, TF'_{canal} is the transfer function between the pressure at the inner microphone and the pressure that would be measured at the eardrum for the occluded ear, TF'_{ext} is the transfer function between the pressure measured at the external microphone and the one measured at a microphone located at the centre of the head in the absence of the subject, $TFOE$ is the transfer function of the open ear. Note that all quantities are expressed in decibels. The term $NR^* + TF'_{canal} - TF'_{ext}$ in Eq(2) is referred to as NR and defined as the difference between the SPL at the centre of the head in the absence of the subject and at a microphone at the eardrum location. Eq(2) indicates that if NR^* is known, IL (and therefore $REAT$) can be retrieved by summing up correction terms which need to be determined in some way. These correction factors are usually based on

diffuse field or frontal incidence for hearing protection. The F-MIRE method has been used successfully for continuous measurements on earmuffs in real field environments where the sound field can depart significantly from a diffuse field and may show strong directionalities [4]. These field attenuation measurements have been shown to depend on the direction of the incoming sound, therefore, asking for a revision of the correction factors [5,6]. Gaudreau [5] proposed a finite-element (FE) model of an earmuff coupled with an acoustic test fixture (ATF) exposed to a directional sound field to investigate the angle dependence of NR^*. The model proved to capture adequately the experimental data obtained in a semi-anechoic room for several incidence angles. However, Gaudreau did not investigate the correction factors relating IL and NR^*. While several studies have been made on the influence of the sound incidence on the *TFOE* [7–12], no study has dealt with the other correction factors TF'_{ext}, TF'_{canal} or with the overall correction factor $TF'_{canal} - TF'_{ext} + TFOE$. Obtaining experimentally these factors that depend on both the external and internal microphone positions together with the incidence angle is cumbersome.

The objective of this paper is therefore to use a 3D finite element model of an ATF with and without an earmuff (EAR1000 model) , excited acoustically at various angles of incidence to calculate IL , and NR^* and the various correction factors. Besides providing a tool to understand finely the acoustical behavior of the system, another advantage of this model is that each individual correction factor can be calculated readily individually to determine their relative importance. $TFOE$ can be obtained from the ATF model without earmuff but also from the ATF model with earmuff by performing the difference between IL and NR. The global correction factor $TF'_{canal} - TF'_{ext} + TFOE$ can be readily calculated from the difference between IL and NR^*. To assess the validity of the model, the simulated attenuation results are compared with experimental measurements on an ATF equipped with an earmuff placed in an anechoic room for various incidence angles. The effects of the angle of incidence on the correction factors for specific positions of the external and internal microphones are then discussed.

Knowing how the sound attenuation of an earmuff is affected by the directionality of the incoming sound field may give feedback to manufacturers to improve the acoustical design of their products in these conditions. Angle of incidence dependent correction factors in Eq(2) can be helpful to evaluate the real attenuation of the earmuff when the direction of the exciting sound field is known (e.g using beam forming source localization technique) and help choosing a better HPD for the worker if the sound attenuation is not sufficient. The paper is organized as follows. First, the finite element model and the methodology are described. Second, the experimental set-up is presented. Third, the validity of the model is assessed based on comparisons with experimental data. Finally, an example of the variation of correction factors as a function of the angle of incidence and frequency for specific positions of the external and internal microphones is presented.

2 Modeling strategy and methodology

The modeled configurations are depicted in Figure 1. It consists of an ATF coupled (Figure 1(a))

or not (Figure 1(b)) with an earmuff through a silicone pad which simulates the external flesh in contact with the earmuff. The ATF and earmuff CAD correspond to a G.R.A.S CB-45® (GRAS Sound & Vibration, Denmark) and an EAR1000 model® (3M Hearing Protection, U.S.A.), respectively. The earmuff is made up of five components (i) the plastic earcup, (ii) the comfort cushion, (iii) a rubber plug that links the plastic earcup to (iv) the headband and (v) the sound absorbing foam pad. In this study, only the first four components are considered, the foam pad being ignored. The ear canal in the ATF is a circular cross section cylinder surrounded by a silicone cylindrical ring layer which mimics the skin part in contact with the ear canal. The EC is terminated by a tympanic membrane which acts as a locally reacting boundary impedance condition (eardrum part of the IEC711 coupler impedance [13]). Fixed boundary conditions are applied on the outer lateral boundaries of the silicone pad and ring. The system is excited acoustically by a spherical wave generated by a monopole located at various positions on a sphere of radius 1m centered at the middle of the segment joining the two centers of the tympanic membrane. The positions of the monopole correspond to elevation angles of θ=90° and +45° and azimuthal angles ranging from ϕ=0° to 345° degrees with 30 degree steps for θ=+45° and 15 degree steps for θ=90°, ϕ=0° being the frontal incidence and 270° pointing directly at the right ear. Only the sound transmission through the right earmuff is considered (for the sake of simplicity, the left one is considered as rigid acoustically).

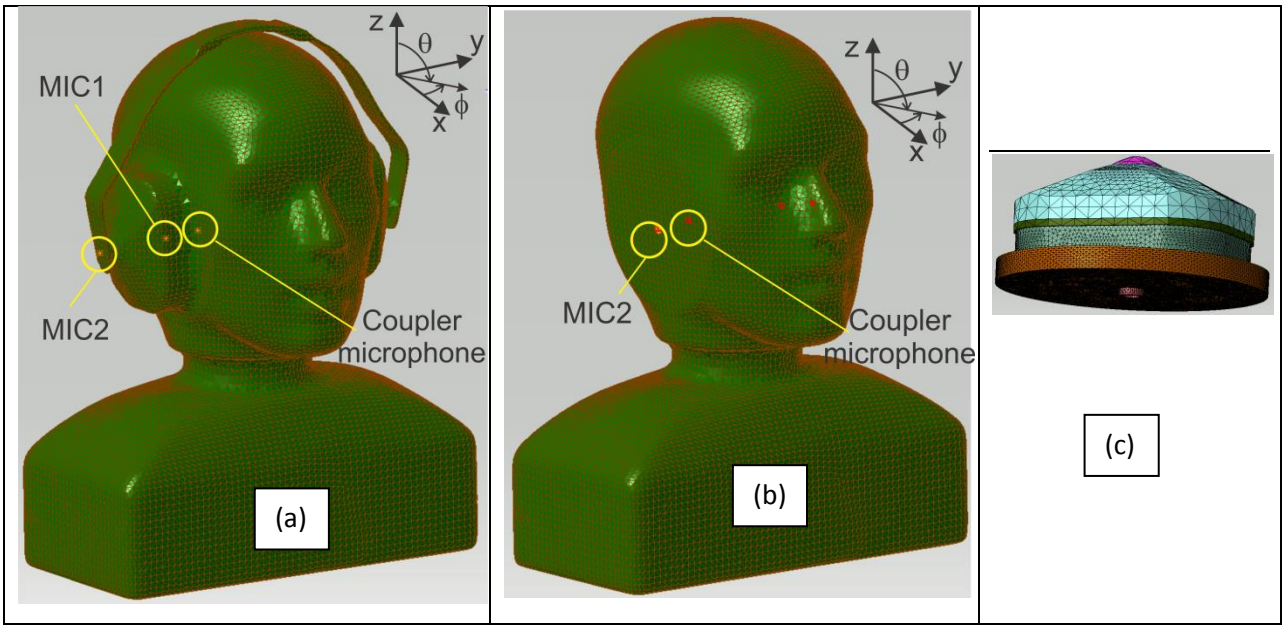

Figure 1: Skin mesh of (a) ATF with earmuff (b) ATF without earmuff (c) Mesh of the plastic shell, comfort cushion, rubber plug, artificial skin pad and ear canal)

The solid domains (earcup, silicone disk, silicone ring) are modeled as elastic isotropic solids The cushion is modeled as an equivalent viscoelastic material with a frequency dependent complex Young's modulus whose values depend on the compression rate of the cushion [14]. The effect of the headband force is accounted for in the model by using an averaged compressed cushion static thickness corresponding to a compression rate of 20.5% and the corresponding cushion mechanical properties [15]. The sound propagation in the external and

internal acoustic domain is governed by Helmholtz equation. Since the external fluid is infinite, a Perfectly Matched Layer condition [16] is applied on the outer boundary of a convex finite acoustic volume surrounding the head/torso/earmuff system to absorb the acoustic waves diffracted by the system. The coupled problem is solved using the Finite Element method. All domains are meshed using 10-noded quadratic tetrahedral based on a meshing criterion of at least 4 elements per wavelength. The details of the FE model are provided in [5]. All the calculations have been carried out with the commercial software Virtual.Lab 13.6® (LMS/SIEMENS, Germany). The properties used for the different domains are summarized in table 1. The model is used to calculate the SPL at the eardrum, at the ear canal entrance for both with and without earmuff ATF conditions. In the case of the ATF with earmuff, the SPL at the centre of the headband (see Figure 2b) is also evaluated in order to calculate NR^*.

Table 1: Physical properties of the various domain

	ρ (kgm^{-3})	E (Pa)	ν	η	c (ms^{-1})	Radius (mm)	Thickness (mm)
Earcup+backplate	1200	1.7e9	0.4	0.05	-		
Cushion	142.8	E(f) see [17]	0.4	0.36	-		10.9
Plug	806	1e8	0.48	0.5	-		
Silicone pad (flesh)	900	340e3	0.48	0.1	-	57.5	10
Silicone ring (skin)	1150	420e3	0.43	0.2	-	5.75	13
Ear canal (air)	1.213	-	-	-	342.2	3.75	27
Air external+internal	1.213				342.2		

3 Experimental set-up

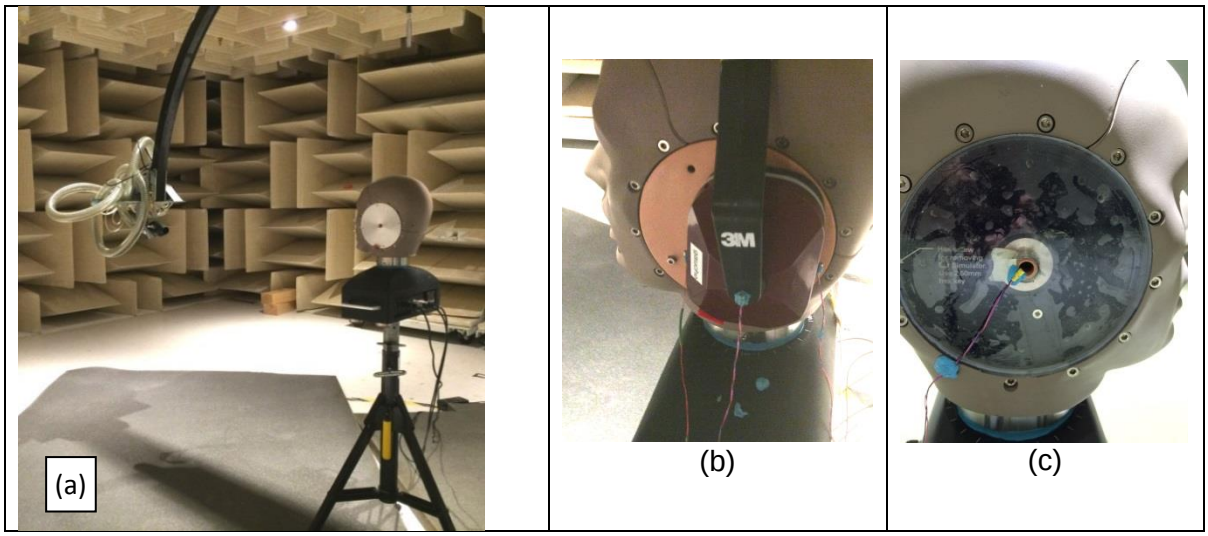

Figure 2: Experimental set-up, sound source revolving around an ATF (no earmuff) in a hemi-anechoic room (homemade aluminum disk on left side) (a) external microphone MIC2 (earmuff with OEM silicone pad) (b) internal microphone MIC1 and homemade silicone pad on right side (c)

In order to evaluate the model, a real G.R.A.S CB-45® ATF equipped or not with an EAR1000 was placed in a hemi-anechoic room at the centre of a motorized arch hanging from the ceiling

(see Figure 2a). The extremity of the arch holds a volume source (VSS210 ©BSWA) directed towards the centre of the head and able to deliver an acoustic power level of 120dB (pink noise). The loudspeaker describes a circle in the two horizontal planes defined by the abovementioned elevation angles. The floor around the ATF was covered with absorbing foam to limit ground reflections. As in the model, the sound absorbing foam was removed from the earcup and the usual silicone pinnae of the ATF were removed and replaced with an aluminum disk on the left side and by a homemade silicone pad on the right side. For the experiment, a microphone (MIC1) was placed inside the earmuff, measuring the internal acoustic pressure close to the ear canal entrance and a second microphone (MIC2), measuring the external acoustic pressure was positioned outside the attachment of the headband (see Figure 2b).

4 Evaluation of the FE model

In order to estimate the global correction factor (defined as the difference between IL and NR^*), the model should be able to predict both IL and NR^*. The proposed FE model has already been assessed regarding NR^* in a simplified version [5]. Gaudreau et al demonstrated that their FE model was able to capture the overall variation of NR^* as a function of the incidence angle. However, no assessment was carried out regarding the IL. Therefore, Figure 3 shows the comparisons between predicted and measured 1/3rd octave band IL for the protected right ear and selected incidence angles. Figure 3 indicates that the model allows for capturing fairly well the frequency dependence of IL. However, there are still several frequency zones where there are amplitude discrepancies between the model and experimental data. There is a reduction of performance in the 400Hz frequency band for the model which is not observed in the measurement. No physical explanation for this peak has been found yet. The largest discrepancies are observed in the mid and the high frequency range and depend on the incidence angle. Similar conclusions are obtained for other incidence angles. Figure 4 displays the comparisons between predicted and measured 1/3rd octave band global correction factor $IL - NR^*$ for the protected right ear and selected incidence angles. Overall, the model captures the frequency trends observed in the experimental data with discrepancies less than 2dB below 800Hz and 4dB at mid and high frequencies except in specific frequency bands (ex around 1250Hz for ϕ=90°, 1600Hz for θ=45°, ϕ=90° and 2500Hz for θ=45° and ϕ=270°). At other incidence angles, the amplitude of the compensation factors are smaller. Detailed investigations with the model showed that the mid frequency range is strongly influenced by the earcup-internal cavity coupled modes together with the coupling between the cushion and the backplate [17]. In the high frequency range, the insertion loss is more affected by the modes governed by the internal earmuff acoustic cavity. Differences between the prediction and measurement can be attributed to experimental conditions such as possible parasitic reflections on the floor, errors in the source/ATF positioning and compressed cushion thickness accurate evaluation due to spatial compression inhomogeneities, They can also be attributed to errors in the model such as (i) inadequate model to capture the possible sound transmission phenomena through the cushion that may occur at mid and high frequencies (ii) inadequate physical parameters for the silicone

disks and rings and damping in the system (iii) inaccurate description of the coupling between the backplate and the cushion which is known to influence the acoustical behavior of the system in the frequency range between the zone controlled by the pumping motion and the one controlled by the sound transmission through the earcup.

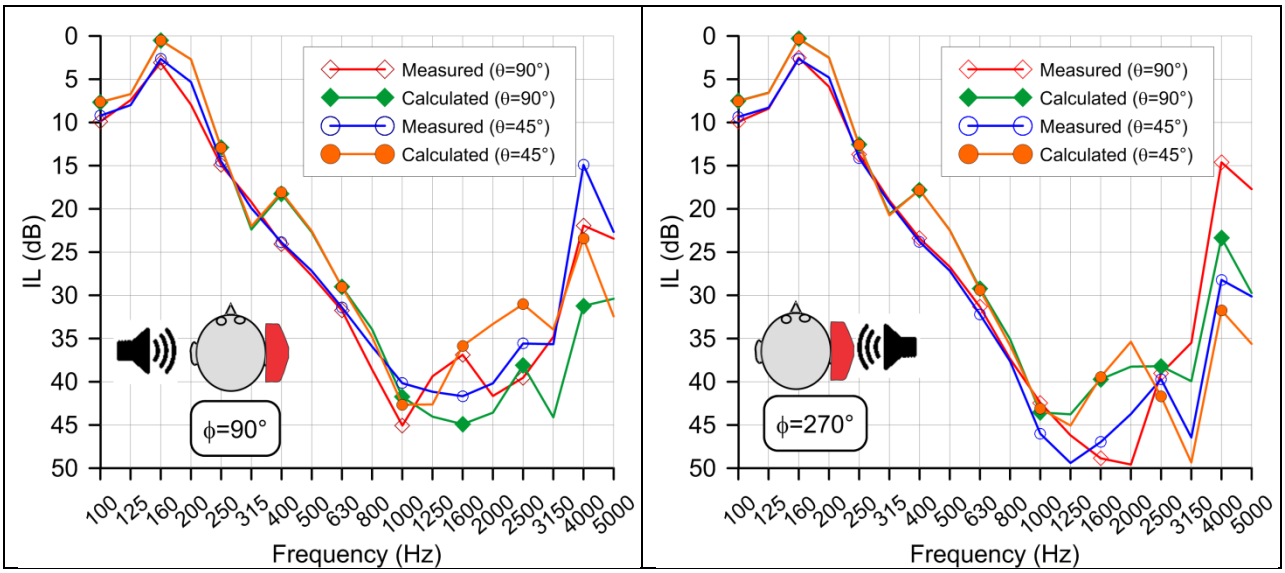

Figure 3: Predicted and measured IL for the right ear earmuff

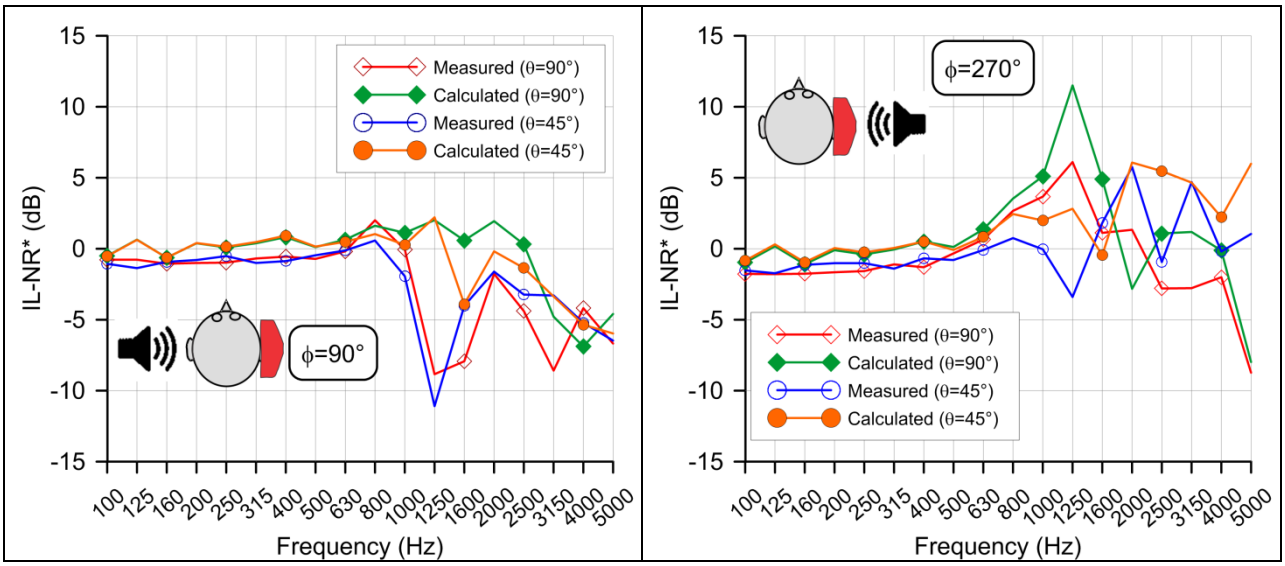

Figure 4: Predicted and measured global correction factors ($IL - NR^*$) for the right ear earmuff

An additional comparison between prediction and experimental data evaluated in the case of the unprotected ATF is shown in Figure 5. This figure compares the predicted and experimental 1/3rd octave bands $TFOE$ s for two elevation angles 90º and 45 º and selected azimuthal angles (frontal, right side). $TFOE$ is defined as the difference between the SPL at the eardrum of the

right ear and at the centre of the head in free field conditions. For the predicted $TFOE$ (figure 1(b)), the silicone pad together with the silicone ring were considered mechanically and acoustically rigid. It is seen that the model and experimental data are in very good agreement (<2dB) for most of the incidence angles. Larger differences are observed at high frequencies for θ=90° and ϕ=90° (ear in shadow region) but overall the model is able to capture the physics very well. Similar correlations were observed for other incidence angles.

Even though there are some discrepancies between the model and the experimental results regarding the IL and the global correction factor, it is interesting to use the model to evaluate individually $TFOE$, TF'_{ext} and TF'_{canal} compared to the global correction factor in order to identify the main contributors as a function of frequency. This is the purpose of next section.

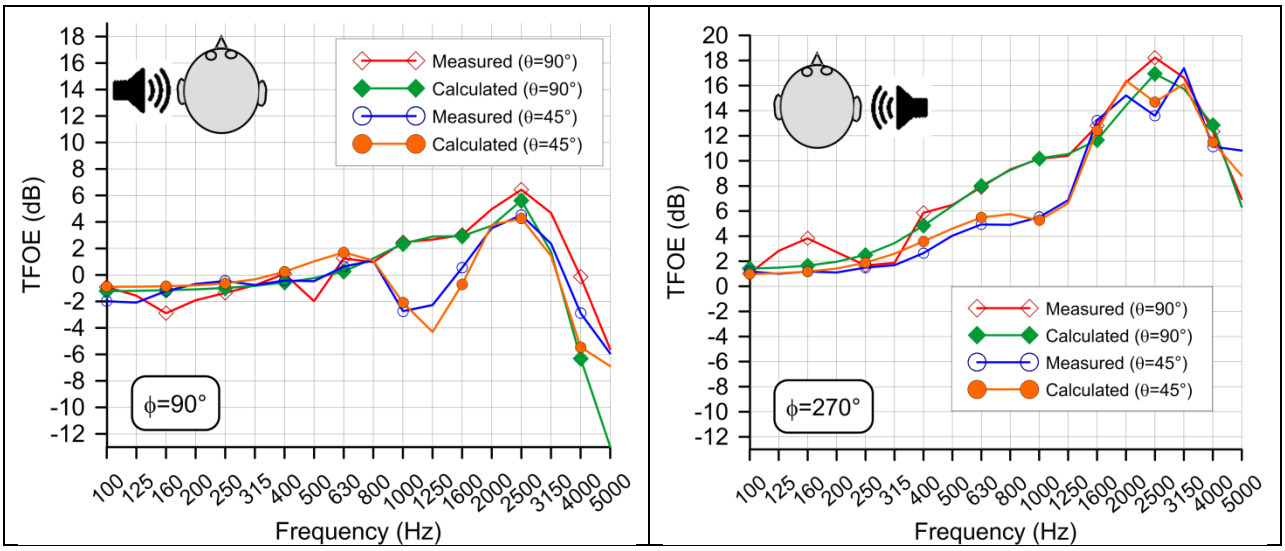

Figure 5: Predicted and measured $TFOE$ s for the right ear

5 Results

Figure 6 plots the calculated $TFOE$, $-TF'_{ext}$ and TF'_{canal} together with the global correction factor $IL - NR^{*}$. First, the global correction factor depends on frequency and incidence angle. It is small at low frequency but can reach values of up to 10dB (negative or positive) at medium and high frequencies depending on the incidence angle. It does not vary monotonously. The largest amplitudes are obtained when the earmuff is in the sunny region (ear exposed directly to the source). Figure 6 shows that TF'_{canal} is always negative and starts to be significant (>3dB) at frequencies above 1250Hz with values up to -12dB. TF'_{ext} and $TFOE$ can be positive or negative depending on frequency. For the earmuff in the shadow region, the magnitude of TF'_{ext} starts to become significant only at high frequencies whereas in the sunny region, it can achieve values of up to 5dB below 1000Hz. The contribution of $TFOE$ can be particularly important in

the shadow region at high frequencies (-13dB) or in the sunny region with values between 5 and 17dB above 400Hz.

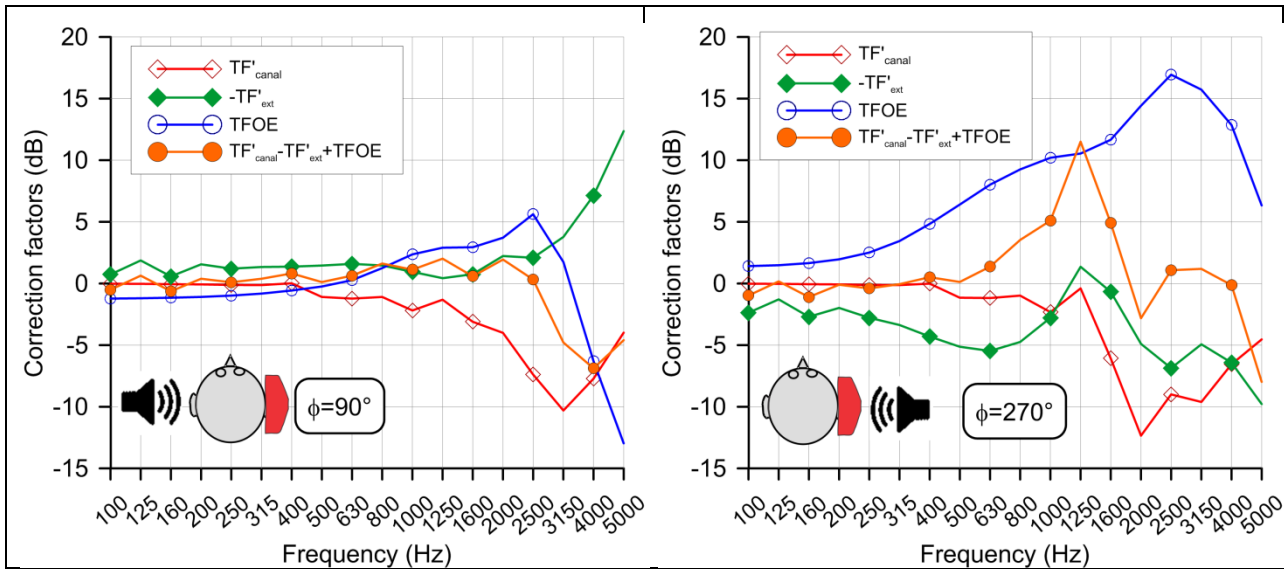

Figure 6: Contributions of $TFOE$, $-TF'_{ext}$ and TF'_{canal} to global correction factor for the right ear

6 Conclusions

In this paper, a 3D finite element model of an ATF with and without an earmuff, excited acoustically at various angles of incidence has been developed to calculate the earmuff IL and NR^* together with various correction factors relating these two indicators. The model has been assessed using a dedicated experimental set-up. Overall the proposed FE model gives the trends for the IL and the global correction factor $IL - NR^*$ even though discrepancies at mid and high frequencies due to possible causes mentioned previously were observed. There is some working progress to better understand and reduce these discrepancies. Depending on the incidence angles and the frequency bands, both measurements and model prediction show that the global correction factor can reach important values (positive or negative), mainly at mid and high frequencies. In addition, the model has been used to quantify the relative importance of each contributor namely $TFOE$, TF'_{ext} and TF'_{canal} as a function of frequency and incidence angle. Besides confirming that the sound attenuation performance of earmuff depends on the incidence angle, this work demonstrates that if an NR-based measurement technique is used to evaluate sound attenuation on the field, it is important to use incidence angle and frequency dependent correction factors to relate NR^* and IL.

Acknowledgments

The authors want to thank IRSST for its financial support.

References

[1] Berger E.H., Royster L.H.; Driscoll. D.P. *The noise manual*, AIHA Press, 2003.
[2] Berger E.H. "Preferred Methods for Measuring Hearing Protector Attenuation," *Proceedings of the Internoise 2005*, Rio de Janeiro, Brazil: Institute of Noise Control Engineering (INCE), 2005.
[3] Nélisse, H. *et al*. "Systematic evaluation of the relationship between physical and psychoacoustical measurements of hearing protectors' attenuation," *Journal of Occupational and Environmental Hygiene*, Vol.12, 2015, pp 829–844.
[4] Nélisse, H. *et al*. Measurement of hearing protection devices performance in the workplace during full-shift working operations, *Ann. Occup. Hyg*, Vol.56 (2), 2012, pp 221–232.
[5] Gaudreau M.A. *Continuous F-MIRE measurement of hearing protectors' attenuation: field measurements and finite element model (in french)*, Ph.D. thesis, École de Technologie Supérieure, 2016.
[6 Le Cocq C. *et al.* Influence of source location, subjects and HPD size on the sound field around earmuffs, *Canadian Acoustics*, Québec: 2011, pp 98–99.
[7] Hammershoi D.; Møller H. "Sound transmission to and within the human ear canal," *The Journal of the Acoustical Society of America*, Vol.100 (1) , 1996, pp 408–427.
[8] Cheng C.I.; Wakefield G.H. "Introduction to head-related transfer functions (HRTFs): Representations of HRTFs in time, frequency, and space," *Journal-Audio Engineering Society*, Vol.49 (4) , 2001, pp 231–249.
[9] Møller H.; *et al.* "Transfer Characteristics of Headphones Measured on Human Ears," *J. Audio Eng. Soc*, 43 (4) , 1995, pp 203–217.
[10] Takane S.; *et al.* "A database of Head-Related Transfer Functions in whole directions on upper hemisphere," *Acoustical Science and Technology*, Vol.23 (3) , 2002, pp 160–162.
[11] Kreuzer W.; Majdak P.; Chen Z. "Fast multipole boundary element method to calculate head-related transfer functions for a wide frequency range," *The Journal of the Acoustical Society of America*, Vol.126 (3) , 2009, pp. 1280–1290.
[12] Gumerov N.A.; *et al*, "Computation of the head-related transfer function via the fast multipole accelerated boundary element method and its spherical harmonic representation," *The Journal of the Acoustical Society of America*, Vol.127 (1) , 2010, pp 370-386,
[13] Viallet G.; Sgard F.; Laville F. "Axisymmetric versus three-dimensional finite element models for predicting the attenuation of earplugs in rigid walled ear canals," *Journal of the Acoustical Society of America*, Vol.134 (6) , 2013, pp 4470–4480.
[14] Boyer S. *Study of the sound transmission through earmuffs: numerical modeling and experimental validation (in french)*, Ph.D.thesis, École de technologie supérieure, 2015.
[15] Boyer, S.; *et al.* "Low Frequency Finite Element Models of the Acoustical Behavior of Earmuffs," *The Journal of the Acoustical Society of America*, Vol.137 (5) , 2015, pp 2602–2613.
[16] Hu, F.Q. "On Absorbing Boundary Conditions for Linearized Euler Equations by a Perfectly Matched Layer," *Journal of Computational Physics*, Vol.129 (1), 1996, pp 201–219.
[17] Boyer, S.; *et al.* "Objective assessment of the sound paths through earmuff components," *Applied Acoustics*, Vol.83 (C) , 2014, pp 76–85.